Progress In Electromagnetics Research Letters, Vol. 22, 59–69, 2011

IMPROVED COMPOSITE RIGHT/LEFT-HANDED CELL FOR LEAKY-WAVE ANTENNA

A. Anghel and R. Cacoveanu

Faculty of Electronics, Telecommunications
and Information Technology
University POLITEHNICA of Bucharest
1-3 Iuliu Maniu, Bucharest 061071, Romania

Abstract—An improved composite right/left-handed (CRLH) unit cell optimized for a leaky-wave (LW) antenna is presented. This CRLH cell consists of a series of one transmission line, an interdigital capacitor, another transmission line and a shunt shorted stub. Introducing the transmission lines, the parasitic self-resonances of the capacitor are shifted outside the operational band, the radiation range is extended and the transition frequency at which the balanced cell condition is achieved can be chosen in the design process from a broader range of frequencies. The characteristics and performances of the proposed cell are verified by simulation and by measuring two artificial transmission lines.

1. INTRODUCTION

The equivalent circuit of the classical CRLH unit cell consists of an impedance constituted by a right-handed (RH) inductance L_R in series with a left-handed (LH) capacitance C_L and of an admittance constituted by a RH capacitance C_R in parallel with a LH inductance L_L. For a balanced cell, the series ω_{se} and shunt ω_{sh} resonances are equal to the transition frequency ω_0. If the CRLH transmission line is not shielded, it radiates and can be used as an antenna [1]. The wave number of the structure has both negative and positive values, so it supports scanning from backfire to endfire [2]. A cell with similar behavior to that of the described CRLH equivalent circuit can be

Received 18 October 2010, Accepted 9 March 2011, Scheduled 23 March 2011
Corresponding author: Andrei Anghel (andreianghel2005@yahoo.com).

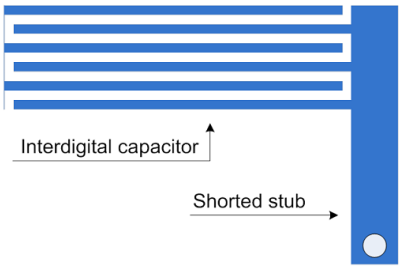

Figure 1. Classical microstrip CRLH cell.

built in microstrip technology using an interdigital capacitor and a shunt shorted stub. The classical microstrip CRLH unit cell proposed in [3] is shown in Figure 1. This cell has one major drawback that in some applications may become very important: self-resonances due to the multiconductor nature of the interdigital capacitor can occur within the desired operational band. An expensive solution to this problem is given in [4] by using bonding wires across the alternate fingers of the capacitor. Other solutions are achieved in different approaches: coplanar-waveguide CRLH cell [5], Metal-Insulator-Metal (MIM) capacitors [6] or edge coupled microstrip lines [7]. This paper presents a new type of microstrip CRLH cell that solves the self-resonances problem in a different manner.

2. IMPROVED MICROSTRIP CRLH CELL BASICS

The resonances of the interdigital capacitor occur at lower frequencies (approaching the operational band) as the capacitance increases (which means an increase of the capacitor's length for a constant number of fingers) [8]. By constraining the length of the capacitor, the maximum values for the LH capacitance $C_L^{\max}$ and RH inductance $L_R^{\max}$ are also constrained, which yields in a lower limit of the series resonance $\omega_{se}^{\min} = 1/\sqrt{L_R^{\max} C_L^{\max}}$. So, in some cases, the cell can't be balanced at the desired transition frequency. The improved CRLH unit cell shown in Figure 2 consists of an interdigital capacitor with two additional transmission lines and a stub shorted through a via to the ground. Introducing the transmission lines, the RH elements are increased (the series inductance and the shunt capacitance) without a further increase of the capacitor's length. As a result, the series and shunt resonances of the cell can be expressed in terms of the length of the transmission lines l_t and their inductance/capacitance per unit-length (L' and C',

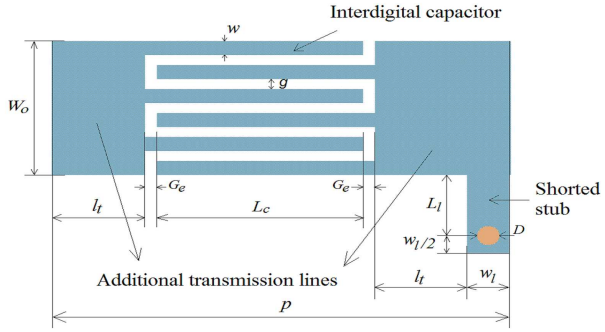

Figure 2. Improved microstrip CRLH cell.

respectively):

$$\omega_{se} = \frac{1}{\sqrt{(L_R^{\max} + 2L'l_t)C_L^{\max}}} \tag{1}$$

$$\omega_{sh} = \frac{1}{\sqrt{L_L^s(C_R^0 + 2C'l_t)}} \tag{2}$$

where L_L^s is the shunt LH inductance given by the stub and C_R^0 is the shunt RH capacitance of the cell with no additional lines. Thus, the transition frequency at which the balanced cell condition is obtained can be brought to lower values only by increasing the length of the transmission lines.

The backfire and endfire frequencies can be obtained from the theoretical dispersion diagram given in [1]. The radiation range is situated between these two limits and can be roughly written as a fractional bandwidth which depends on l_t:

$$FBW = \frac{1}{\sqrt{1 - \frac{\pi B(p^{\max}+2l_t)}{c_o}}} - \frac{1}{\sqrt{1 + \frac{\pi B(p^{\max}+2l_t)}{c_o}}} \tag{3}$$

here, $p^{\max}$ is the maximum length of the initial cell at which no parasitic resonances occur in the desired band, B is the passband of the resulting CRLH transmission line and c_o is the speed of light in vacuum. Consequently, the radiation range is increased proportional to the length of the additional lines at a constant passband. However, the classical cell can be balanced if we accept a distorted phase characteristic, but with a narrower radiation range due to the smaller increase in length (mainly given by the capacitor) compared to the length of the additional lines. As second order effects, in the design

of a balanced cell, both the variation of the capacitor finger's length from the initial value and the increase of the LH capacitance should be taken into account.

3. DESIGN AND OPTIMIZATION PROCESS

The initial values for the main parameters of the unit cell are chosen as follows: the number of fingers of the capacitor for microstrip implementation may be technologically limited in some situations by the minimum spacing between two adjoining elements, the length of the capacitor is set according to the desired transition frequency, but should not exceed the maximum value at which there are no parasitic resonances in the operational band and the length of the transmission lines is set to a small value (e.g., 0.01 mm). The final parameters of the designed cell are obtained by optimization based on the gradient method and an additional fine tuning. The variables used in the optimization algorithm are: the length of the capacitor's finger L_c, the length L_l of the stub which has a higher limit due to the condition of a non-dispersive inductance and the length of the transmission lines l_t that can increase up to a quarter of the finger's optimized length (in order to maintain the metamaterial homogeneity condition $p < \lambda_g/4$, where p is the cell length and λ_g the guided wavelength [1]). The optimization target is a cell with total transfer and zero phase shift at the transition frequency ω_0 which in terms of S parameters means:

$$|S_{11}(\omega_0)| < -20\,\mathrm{dB} \tag{4}$$

$$\arg(S_{21}(\omega_0)) = 0 \tag{5}$$

Onward, the resulting optimized parameters are adjusted by making a trade-off between the well balanced cell and the desired radiation range. This range can be graphically determined as the solution for:

$$\left|\frac{\beta(\omega)}{k_0}\right| < 1 \tag{6}$$

where β is the guided propagation factor, ω is the frequency and $k_0 = \omega/c$ is the free space wave number [2]. The fine tuning process is accomplished by full-wave simulation (employing the method of moments), taking into account the thickness of the metallization layer and the finite conductivity of copper. Additionally, the presence of the transmission lines adds a new degree of freedom for balancing the unit cell.

In order to emphasize the improvements of the new cell, a classical CRLH cell and an improved cell were both designed and optimized

imposing the transition frequency at about 3.7 GHz and the radiation range of at least 2 GHz.

4. EXPERIMENT AND SIMULATION

4.1. Test Prototypes

To verify the predicted unit cell, two experimental microstrip CRLH transmission lines (with 10 and respectively 20 cells) were built and measured. The prototypes shown in Figure 3 were fabricated on a Rogers 3003 substrate with a 1.524 mm thickness. The feeding line has 3.80 mm width which corresponds to a characteristic impedance of 50 Ω. To obtain minimal return loss, the circuits are made reciprocal by terminating them with shunt shorted stubs that have modified dimensions corresponding to a symmetric unit cell [2].

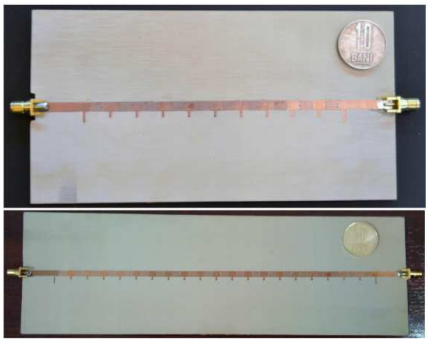

Figure 3. CRLH artificial line prototypes.

4.2. Results

The dimensions of both cells (improved and classical) are presented in Table 1. A plot of the propagation β and attenuation α factors for the designed unit cell versus the optimized classical cell is shown in Figure 4.

When using the improved cell, the effects of the parasitic resonances are eliminated from the passband and the radiation range is extended by 24% (for the classical cell is between 3.04–4.96 GHz and for the improved one between 3.02–5.40 GHz). The homogeneity condition for both cells is satisfied in the whole radiation range (for the highest frequency this condition states $p < 14$ mm). It can be seen that using the specified substrate in this range of frequencies, the resulting series

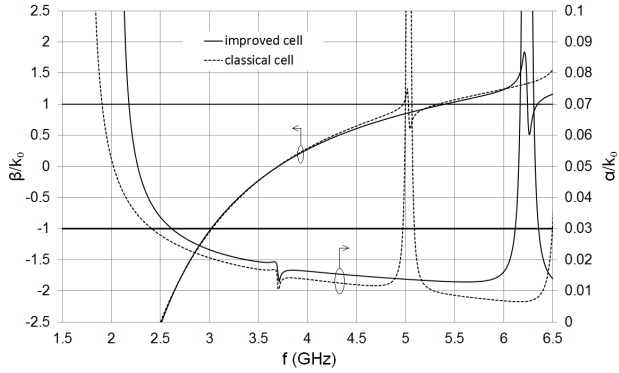

Figure 4. Propagation and attenuation factors normalized to k_0.

Table 1. Dimensions of the improved and classical cells.

Parameter(mm)/Cell type	Improved	Classical
L_c (capacitor finger length)	4.88	6.41
l_t (length of the transmission lines)	2.18	-
G_e (gap finger-line)	0.28	0.28
w (capacitor finger width)	0.40	0.40
g (gap between fingers)	0.28	0.28
W_o (feeding line width)	3.80	3.80
L_l (stub length)	1.72	2.79
w_l (stub width)	1.00	1.00
D (via diameter)	0.50	0.50
p (unit cell length)	10.80	7.97

resonance can't be obtained using the classical cell without a distortion effect on the dispersion diagram. The fact that the propagation factor has negative values proves the LH nature of the proposed cell.

The Bloch impedance of the designed cell (computed with the expression given in [1]) is shown in Figure 5. Its real part is around $30\,\Omega$ in the radiation range (not far from the characteristic impedance, so the matching is not difficult) and the discontinuity at the transition frequency is acceptable.

The prototypes are used as a proof of concept. The return and insertion losses for the 10-cell prototype are shown in Figure 6. The

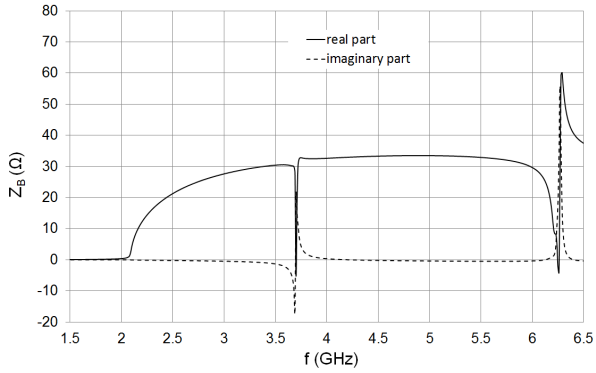

Figure 5. The Bloch impedance of the designed cell.

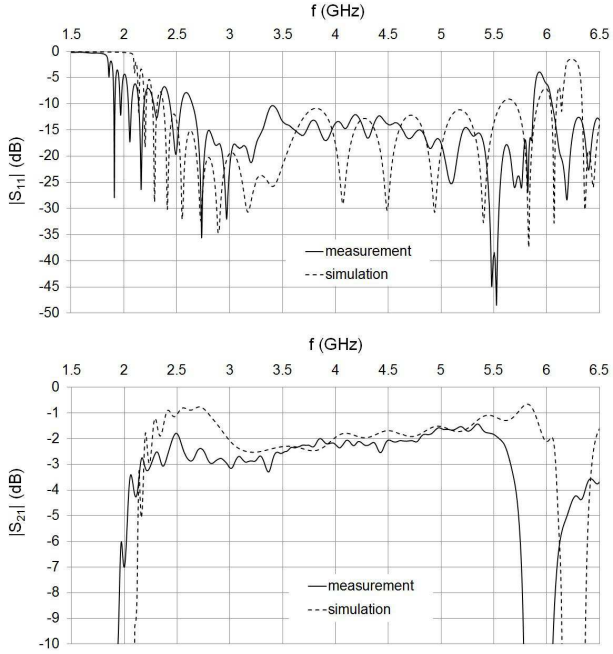

Figure 6. Return and insertion losses for the 10-cell prototype.

high value of the insertion loss (about −2 dB) shows that only around one third of the power is radiated while the rest is absorbed by the matched load. As expected, the artificial transmission line behaves as a filter with a passband similar to that of the cell, with almost

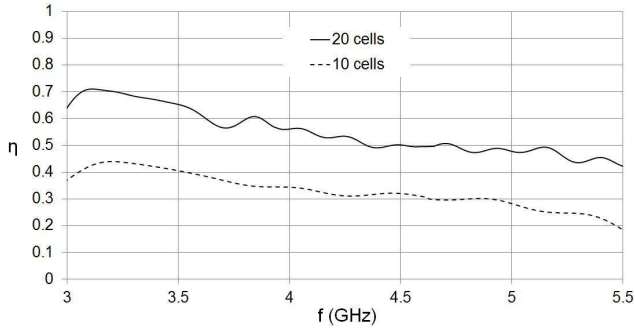

Figure 7. Efficiency versus frequency for the two prototypes.

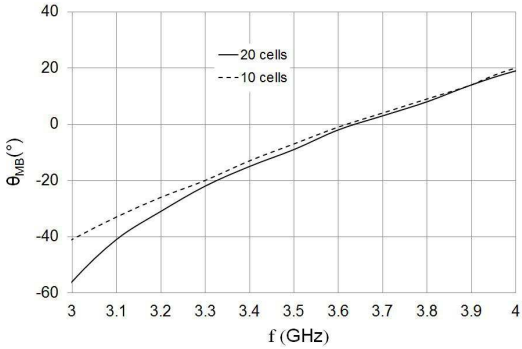

Figure 8. Scanned angle versus frequency for the LW antennas.

no gap at the transition frequency (which proves that the line is well balanced). The band obtained by measurement is slightly different than the simulated result (with 6% from the central frequency). The comparison of the measured and predicted insertion loss shows good agreement in the radiation range (roughly between 3–5.4 GHz).

Figure 7 shows the efficiency η in the radiation range for the two antennas. The 20-cell prototype radiates more power than the smaller 10-cell antenna (50–60% efficiency compared to 30–40%) due to its increased length (which means more space for power leakage). In order to emphasize the LH nature of the antenna prototypes, the angle of the main beam θ_{MB} in the E-plane was measured at different frequencies. The results are shown in Figure 8.

5. CONCLUSION

An improved CRLH cell is introduced. Compared to the classical cell, this newly designed unit cell has certain advantages: the parasitic self-resonances of the interdigital capacitor are eliminated from the passband, the transition frequency can be chosen from a broader range, the radiation band is increased and the cell can be more easily balanced using the length of the transmission lines as a new degree of freedom.

APPENDIX A. PROOF OF THE FRACTIONAL BANDWIDTH RELATION

The propagation factor as a function of frequency $\beta(\omega)$ for a balanced unit cell of physical length p can be expressed as:

$$\beta(\omega) = \frac{1}{p}\left(\frac{\omega}{\omega_R} - \frac{\omega_L}{\omega}\right) \tag{A1}$$

with the variables $\omega_R = 1/\sqrt{L_R C_R}$ and $\omega_L = 1/\sqrt{L_L C_L}$. The theoretical backfire and endfire frequencies can be obtained by solving the equations:

$$\beta(\omega_{BF}) = -k_0 \tag{A2}$$

$$\beta(\omega_{EF}) = +k_0 \tag{A3}$$

The fractional bandwidth is expressed as:

$$FBW = \frac{\omega_{EF} - \omega_{BF}}{\omega_0} = \frac{1}{\sqrt{1 - \frac{\omega_R p}{c_o}}} - \frac{1}{\sqrt{1 + \frac{\omega_R p}{c_o}}} \tag{A4}$$

According to [1] the LH highpass and RH lowpass cutoff frequencies for a CRLH network of balanced cells take the forms:

$$\omega_{cL}^{bal} = \omega_R\left(\sqrt{1 + \frac{\omega_L}{\omega_R}} - 1\right) \tag{A5}$$

$$\omega_{cR}^{bal} = \omega_R\left(\sqrt{1 + \frac{\omega_L}{\omega_R}} + 1\right) \tag{A6}$$

The passband can be written as:

$$B = \frac{\omega_{cR}^{bal} - \omega_{cL}^{bal}}{2\pi} = \frac{\omega_R}{\pi} \tag{A7}$$

so it depends only on ω_R. The expression given in Equation (3) for the FBW is easily obtained by combining Equations (A4) and (A7) and expressing the length of the cell as $p = p^{\max} + 2l_t$.

APPENDIX B. DERIVATION OF THE PROPAGATION AND ATTENUATION FACTORS OF THE CRLH CELL FROM THE *S* PARAMETERS

The complex propagation factor $\gamma = \alpha + j\beta$ for a cell of length p may be obtained from [1, 9]:

$$\cosh(\gamma p) = \frac{1 - S_{11}S_{22} + S_{12}S_{21}}{2S_{21}} \tag{B1}$$

The function $\cosh^{-1}$ for complex quantities is not easy to compute. So, this complex relation should be written as two real equations. For notation simplicity, we introduce two additional variables:

$$x = \mathrm{Re}\{\cosh(\gamma p)\} = \cosh(\alpha p)\cos(\beta p) \tag{B2}$$

$$y = \mathrm{Im}\{\cosh(\gamma p)\} = \sinh(\alpha p)\sin(\beta p) \tag{B3}$$

which can be expressed from (B1) in terms of S parameters. Now α and β can be obtained using real inverse functions ($\cosh^{-1}$ and $\cos^{-1}$, respectively):

$$\alpha p = \cosh^{-1}\left(\sqrt{\frac{1+x^2+y^2}{2} + \sqrt{\left(\frac{1+x^2+y^2}{2}\right)^2 - x^2}}\right) \tag{B4}$$

$$\beta p = \cos^{-1}\left(\sqrt{\frac{1+x^2+y^2}{2} - \sqrt{\left(\frac{1+x^2+y^2}{2}\right)^2 - x^2}}\right) \tag{B5}$$

In order to have a continuous function $\beta(\omega)$, the discontinuities of βp are eliminated using a phase unwrapping procedure.

REFERENCES

1. Caloz, C. and T. Itoh, *Electromagnetic Metamaterials: Transmission Line Theory and Microwave Applications*, John Wiley & Sons, New Jersey, 2006.
2. Lai, A., C. Caloz, and T. Itoh, "Dominant mode leaky-wave antenna with backfire-to-endfire scanning capability," *Electronics Letters*, Vol. 38, No. 23, 1414–1416, Nov. 2002.
3. Caloz, C. and T. Itoh, "Transmission line approach of left-handed (LH) materials and microstrip implementation of an artificial LH transmission line," *IEEE Transactions on Antennas and Propagation*, Vol. 52, No. 5, 1159–1166, May 2004.

4. Sánchez-Martínez, J., J., E. Márquez-Segura, P. Otero, and C. Camacho-Peñalosa, "Artificial transmission line with left/right-handed behavior based on wire bonded interdigital capacitors," *Progress In Electromagnetics Research B*, Vol. 11, 245–264, 2009.
5. Liu, C. Y., Q. X. Chu, and J. Q. Huang, "Double-side radiating leaky-wave antenna based on composite right/left-handed coplanar-waveguide," *Progress In Electromagnetics Research Letters*, Vol. 14, 11–19, 2010.
6. Monti, G., R. de Paolis, and L. Tarricone, "Design of a 3-state reconfigurable CRLH transmission line based on MEMS switches," *Progress In Electromagnetics Research*, Vol. 95, 283–297, 2009.
7. Abdelaziz, A., F., T. M. Abuelfadl, and O. L. Elsayed, "Leaky wave antenna realization by composite right/left-handed transmission line," *Progress In Electromagnetics Research Letters*, Vol. 11, 39–46, 2009.
8. Casares-Miranda, F. P., P. Otero, E. Márquez-Segura, and C. Camacho-Peñalosa, "Wire bonded interdigital capacitor," *IEEE Microwave and Wireless Components Letters*, Vol. 15, No. 10, 700–702, Oct. 2005.
9. Pozar, D. M., *Microwave Engineering*, John Wiley & Sons, New York, 1998.